



OPTIMAL PHOTOVOLTAIC WATER PUMPING SYSTEM PERFORMANCE UNDER DIFFERENT OPERATING CONDITIONS

G. El-Saady¹, El-Nobi A. Ibrahim², Mostafa Ahmed³

Electrical Engineering Department, Faculty of Engineering, Assiut University, Assiut, Egypt

(Received 17 January 2015; Accepted 17 February 2015)

ABSTRACT

This paper presents dc photovoltaic pumping system. The system consists of photovoltaic (PV) generator, boost converter and permanent magnet (PM) dc motor-pump set. Each part of the system is modelled. Photovoltaic generator parameters are extracted based on data-sheet parameters. Boost converter is designed to operate in continuous conduction mode (CCM) and controlled using incremental conductance (IC) algorithm for maximum power point tracking (MPPT). The system is simulated using Matlab/Simulink. The proposed system is studied under direct coupling and maximum power point tracking conditions. The results show a very good performance MPPT compared with direct coupling. The system is tested under varying conditions of temperature and radiation.

Keywords: *PV generator, pumping system, dc-dc boost converter and MPPT.*

1. Introduction

One of the most important applications of photovoltaic (PV) standalone systems is for water pumping, particularly in rural areas that have a considerable amount of solar radiation and no access to national grids [1]. Since the photovoltaic generators are dc sources, these generators are very useful to supply dc motors. When a dc motor is directly connected to a photovoltaic module (PVM), the operating point of the PVM is very far from its maximum power point (MPP)[2,3].

Many MPPT methods have been developed and implemented, which vary in complexity, sensors required, convergence speed, cost, range of effectiveness, implementation hardware, popularity, and other aspects [4]. These methods can be classified into three main categories; model-based algorithms, training-based algorithms, and searching algorithms. Model-based MPPT algorithms refer to those using any mathematical model or look up table model in calculating the maximum power point voltage and/or the maximum power point current [5].

Training-based (Artificial Intelligence) MPPT algorithms including fuzzy logic control and artificial neural networks need prior training data. Searching algorithms, including perturb and

* Corresponding author.

Email address: gaber1@yahoo.com

observe P&O algorithm and IC algorithm, measure the array output current/power or the converter output current/power and utilize the measured parameter to determine whether to increase or to decrease a control parameter. The control parameter can be a reference voltage for the array output voltage or it can be the duty ratio of the switching signal [5].

Searching MPPT algorithms do not require previous knowledge of the PV generator characteristics and do not require measurement of solar intensity and cell temperature [3, 5]. In order to improve system performance a maximum power point tracker using dc-dc power converter as interfacing circuit between PVM and motor-pump set is used. Different types of dc–dc converters have been employed including the buck converter and the boost converter depending on the voltage rating of the motor and the PV array [1]. Selection of the type of dc motor is an important step for operation with a PV source [6].

In this paper, PV generator is modelled with its parameters extracted based on data-sheet and the boost converter is controlled using IC algorithm for maximum power point tracking. The system is studied with and without MPPT and simulated using Matlab program. Boost converter is designed to work in CCM. The steady state solution of the system is reached using simple calculation and has a very good agreement with that obtained using Matlab/Simulink .The system is studied under varying atmospheric conditions of temperature and radiation.

2. Description and modelling of the system

The proposed system consists of photovoltaic array, dc-dc boost converter and a 1-kW PM dc motor-pump set .This system is shown in Fig 1.Boost converter is controlled using direct control method in which the duty ratio of the converter is used directly as the control parameter[7,8] as shown in Fig 2.

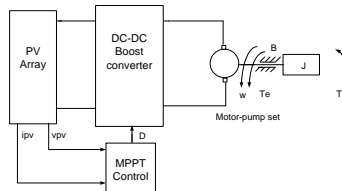


Fig. 1. PV generator feeding PM dc motor-pump set via boost converter

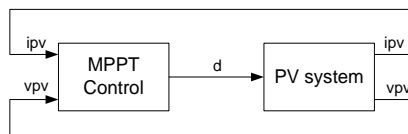


Fig. 2. Direct duty ratio control

2.1. PV model

The PV module current-voltage (I-V) equation based on the single exponential model is given by [9, 10]:

$$i = I_{ph} - I_o \left(\exp \left(\frac{v+i R_s}{n N_s V_t} \right) - 1 \right) - \frac{v+i R_s}{R_{sh}} \tag{1}$$

The mathematical equations of the PV model are developed as follows [9, 10]:

$$V_t = \frac{K T_{stc}}{q} \tag{2}$$

$$I_{ph}(G, T) = \left(I_o(T) \exp\left(\frac{V_{oc}(T)}{n N_s V_t}\right) + \frac{V_{oc}(T)}{R_{sh}} \right) \frac{G}{G_{stc}} \quad (3)$$

$$I_o(T) = \left(I_{sc}(T) - \frac{V_{oc}(T) - I_{sc}(T) R_s}{R_{sh}} \right) \exp\left(-\frac{V_{oc}(T)}{n N_s V_t}\right) \quad (4)$$

$$I_{sc}(T) = I_{sc} + k_i(T - T_{stc}) \quad (5)$$

$$V_{oc}(T) = V_{oc} + k_v(T - T_{stc}) \quad (6)$$

Where:

- V_t - the junction thermal voltage
- I_{ph} - the photo-generated current in standard test conditions(STC)
- I_o - dark saturation current in STC
- R_s - panel series resistance
- R_{sh} - panel parallel (shunt) resistance
- n - diode quality (ideality) factor
- N_s - number of cells in the panel connected in series
- K -Boltzmann's constant(1.38×10^{-23} J/K)
- q -electron charge(1.6×10^{-19} C)
- I_{sc} -short-circuit current in STC
- V_{oc} -open-circuit voltage in STC
- k_i -temperature coefficient of the short-circuit current
- k_v -temperature coefficient of the open-circuit voltage
- G -solar irradiance in W/m^2
- G_{stc} -irradiance under STC($1000W/m^2$)

For simulation, KC200GT module was chosen. Its electrical parameters are tabulated in Table 1.

Table 1.
Parameters of KC200GT module

Maximum power(P_{max})	200.1 W
Voltage at MPP(V_{mpp})	26.3 V
Current at MPP(I_{mpp})	7.61 A
Open circuit voltage (V_{oc})	32.9 V
Short circuit current(I_{sc})	8.21 A
k_i	3.2 mA/°C
k_v	-0.123 V/°C
N_s	54

I_{ph} , I_o , R_s , R_{sh} and n are the five unknown parameters of the model [9]. I_{ph} can be calculated from (3) and I_o from (4). R_s , R_{sh} and n can be calculated using the Newton-Raphson method [11]:

$$R_s = 0.2171\Omega, \quad R_{sh} = 951.9318\Omega \quad \text{and} \quad n = 1.3416$$

2.2. Boost converter model

Fig. 3 shows the equivalent circuit of boost converter. In continuous conduction mode of operation the mathematical equations of the boost converter are given as follows [12, 13]:

$$\frac{V_o}{V_i} = \frac{1}{1 - D} \quad (7)$$

$$\frac{I_o}{I_i} = 1 - D \quad (8)$$

Where:

- V_i -The input voltage
- V_o -The output voltage
- I_o -The output current
- I_i -The input current
- D -The duty cycle

C. PM DC Motor-Pump set Model

PM dc motor can be described as follows [14, 15]:

$$V_a = i_a R_a + L_a \frac{di_a}{dt} + E_b \quad (9)$$

$$E_b = K_b w_m \quad (10)$$

$$T_e = J \frac{dw_m}{dt} + B w_m + T_l \quad (11)$$

$$T_e = K_e i_a \quad (12)$$

Where:

- V_a - armature voltage
- i_a -armature current
- R_a -armature resistance
- L_a -armature inductance
- E_b -motor back-emf
- K_b -back-emf constant(V.sec/rad)
- w_m -motor speed(rad/s)
- T_e -electromagnetic torque(N.m)
- J -moment of inertia(Kg/m^2)
- B -viscous friction coefficient (N.m.sec/rad)
- T_l -load torque(N.m)
- K_e -torque constant(N.m/A)

In case of centrifugal pump load, the load torque can be taken as [16, 17]:

$$T_l = K_p w_m^2 \quad (13)$$

Where K_p is the pump constant ($N.m. (sec/rad)^2$).

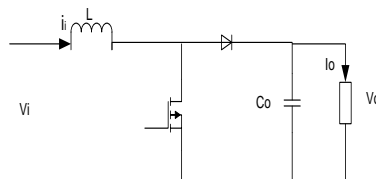


Fig. 3. Equivalent circuit of boost converter

3. Design of MPPT with IC algorithm and boost converter

3.1. MPPT algorithm

IC technique is widely used for MPPT technique. IC based algorithm has advantages over other conventional methods because it is easy to implement, high tracking speed and better efficiency [18]. The incremental conductance method is working on the fact that the slope of the PV array power curve is zero at the MPP, positive on the left of the MPP, and negative on the right, as given by (14):

$$\begin{cases} \frac{dI}{dV} = -\frac{I}{V}, \text{ At MPP} \\ \frac{dI}{dV} > -\frac{I}{V}, \text{ Left of MPP} \\ \frac{dI}{dV} < -\frac{I}{V}, \text{ Right of MPP} \end{cases} \quad (14)$$

Using the rules in (14), the basic flow chart for IC is shown in Fig. 4.

3.2. Boost converter design

The critical inductance, L_c of boost converter is the boundary edge between continuous and discontinuous conduction modes is defined as [12, 13]:

$$L_c = \frac{R D (1 - D)^2}{2 F_s} \quad (15)$$

Value of the inductor required to ensure the converter operating in the continuous conduction mode is calculated from [12, 19]:

$$L \geq \frac{V_o D (1 - D)}{F_s \Delta I_1} \quad (16)$$

The coupling capacitor between the PV module and boost converter is calculated such that the ripple of PV output current must be less than 2 % of its mean value [19]:

$$C_i \geq \frac{I_o D^2}{0.02 (1 - D) V_i F_s} \quad (17)$$

The output capacitor value calculated to give the desired peak-to-peak output voltage ripple is [12, 13]:

$$C_o \geq \frac{V_o D}{\Delta V_o R F_s} \quad (18)$$

Where:

- R- load resistance
- F_s -switching frequency
- ΔI_1 -peak-to-peak ripple of the inductor current
- ΔV_o - peak-to-peak ripple of the output voltage

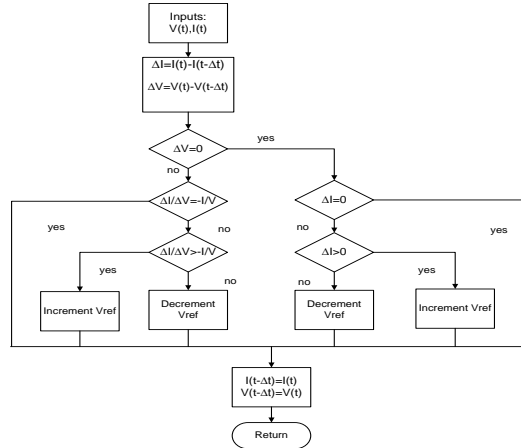


Fig. 4. Basic flow chart of IC method

4. Steady state analysis

Parameters of motor-pump set used in the study are tabulated in Table 2. In case of direct coupling between PV generator and motor-pump set, the system operates at the intersection point between the I-V curve of the PV generator and the load-line. The load-line of motor-pump set is obtained using simulation via applying a ramp voltage to the set at the rate of 1V/S ranging from zero to rated voltage. Fig. 5 shows the operating points of the PV array that consists of 6 modules (3 series modules and 2 parallel with 200 W peak each) with the motor-pump set load-line. The curves are at constant radiation of 1000W/m^2 and changing temperature of 25, 50 and 75°C . Motor-pump set P-V curves at constant radiation of 1000W/m^2 and changing temperature of 25, 50 and 75°C are shown in Fig. 6. It is obvious from the curves that the system operates far from maximum power points which led to lower energy utilization and efficiency.

Results with constant temperature at 25°C and varying radiation of 400W/m^2 , 600W/m^2 , 800W/m^2 and 1000W/m^2 are obtained also. Fig. 7 shows I-V curves and P-V in Fig. 8.

Table 2.

Parameters of motor-pump set

Armature resistance(R_a)	1.254 Ω
Armature inductance(L_a)	3.49 mH
Back-emf constant($K_b = K_e$)	0.333 V.sec/rad
Viscous friction coefficient(B)	0.0008 N.m.sec/rad
Moment of inertia(J)	0.004 Kg/m^2
Armature voltage(V_a)	135 V
Pump constant(K_p)	1.9×10^{-5} N.m. (sec/rad) ²

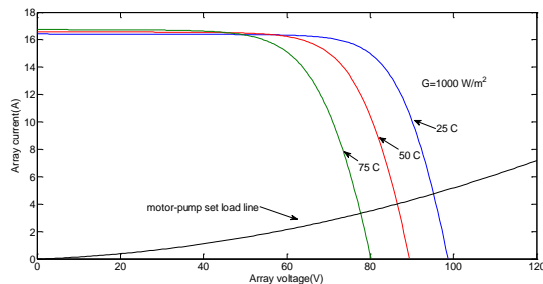


Fig. 5. Array I-V curves with constant radiation and varying temperature

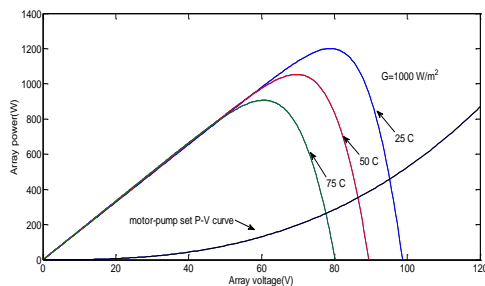


Fig. 6. Array P-V curves with constant radiation and varying temperature

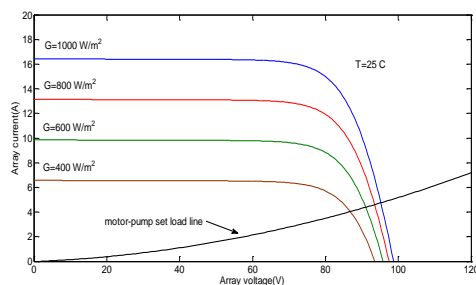


Fig. 7. Array I-V curves with constant temperature and varying radiation

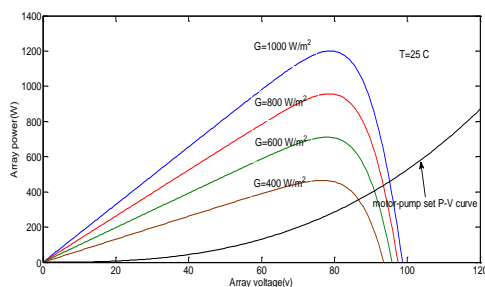


Fig. 8. Array P-V curves with constant temperature and varying radiation

Matlab model for the system is build based on equations (1) to (13) and the results under direct coupling match approximately the expected values from I-V and P- V curves. Array output power, armature voltage and armature current are shown in Figs. 9, 10 and 11 respectively. The results are with constant radiation at 1000W/m^2 and varying temperature of 25, 50 and 75°C . Fig. 12 shows motor speed and Fig. 13 shows the torque under the same conditions stated previously. At the beginning of simulation and with motor accelerating the system operates near the short circuit conditions (back-emf=0), while the

voltage builds up. If the temperature changes this moves the operating point towards the new intersection between the I-V curves of the array and the motor.

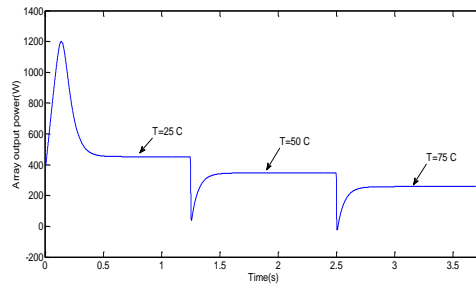


Fig. 9. Array output power response with constant radiation and varying temperature

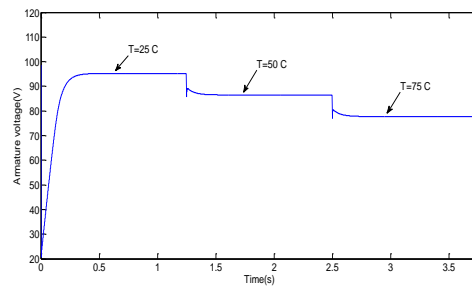


Fig. 10. Armature voltage response with constant radiation and varying temperature

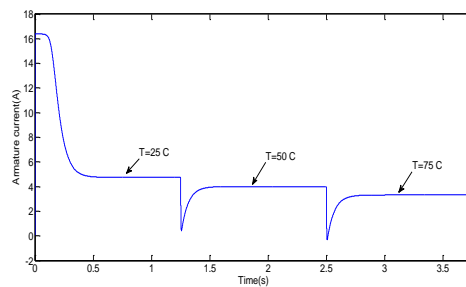


Fig. 11. Armature current response with constant radiation and varying temperature

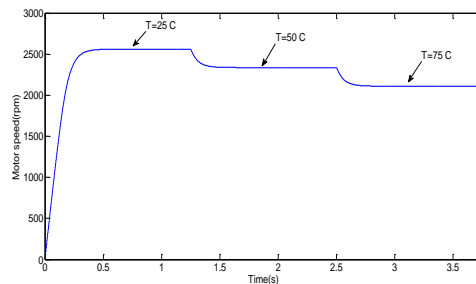


Fig. 12. Motor speed response with constant radiation and varying temperature

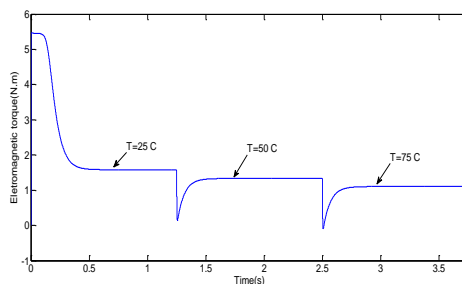


Fig. 13. Torque response with constant radiation and varying temperature

Simulation results with constant temperature at 25 °C and varying radiation of 400W/m², 600W/m², 800W/m² and 1000W/m² are done also. Figs. 14, 15 and 16 show the array output power, armature voltage and armature current. Motor speed and the torque are shown in Figs. 17 and 18.

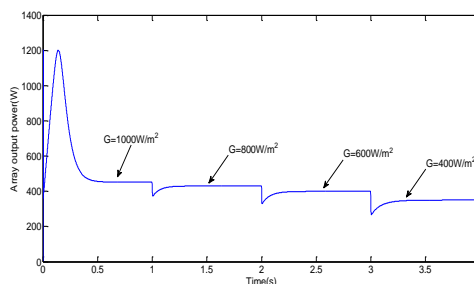


Fig. 14. Array output power response with constant temperature and varying radiation

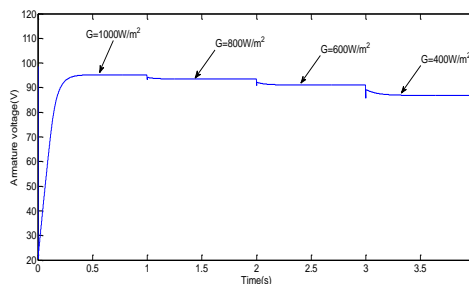


Fig. 15. Armature voltage response with constant temperature and varying radiation

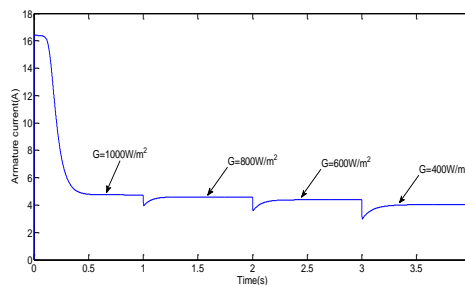


Fig. 16. Armature current response with constant temperature and varying radiation

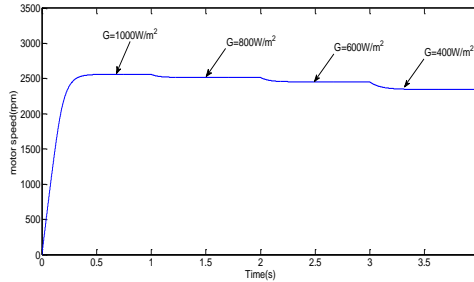


Fig. 17. Motor speed response with constant temperature and varying radiation

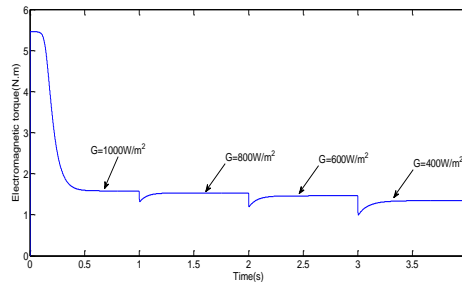


Fig. 18. Torque response with constant temperature and varying radiation

Results with MPPT are obtained, assuming lossless dc-dc boost converter:

$$P_i = P_o = V_i I_i = V_o I_o$$

This equation can be represented by constant power line, by drawing this line with the I-V curves of PV generator and motor-pump set, the operating point of the system can be easily obtained. The proposed system is solved with constant radiation and varying temperature. Also results are obtained with constant temperature and varying radiation. Fig.19 shows constant power lines tangent the I-V curves at maximum power points under constant radiation and varying temperature. With the system operates at MPP, the operating points of the system are the intersection points of motor-pump set load line and constant power lines. Knowing MPP voltages and operating points voltages, the optimum duty cycle ratio can be calculated. Results with constant temperature and varying radiation are shown in Fig.20.

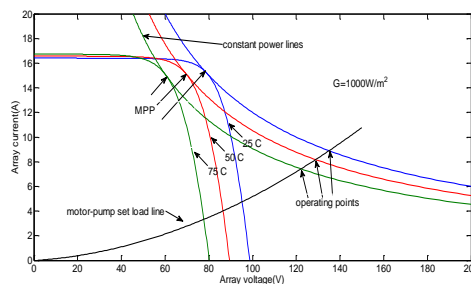


Fig. 19. I-V curves with converter constant power lines under constant radiation and varying temperature

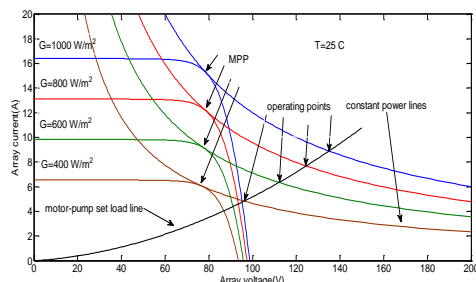


Fig. 20. I-V curves with converter constant power lines under constant temperature and varying radiation

5. Dynamic analysis and simulation results

The Simulink model of proposed system is shown in Fig. 21. The system consists of photovoltaic generator, boost converter and PM dc motor pump set .System model is based on equations (1) to (13) .Boost converters is controlled using IC method, its parameters are designed using equations (16) to (18). The parameters of the boost converter are calculated and tabulated in Table 3.

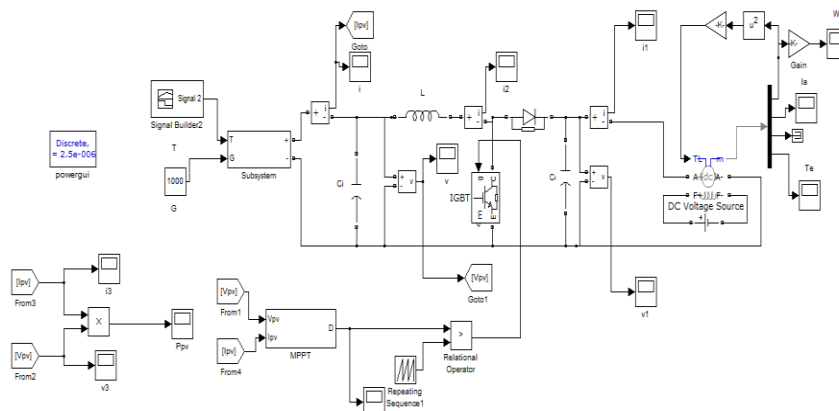


Fig .21. Simulink model of the system

Table 3.
Parameter of boost converter

$L(\text{mH})$	5
$C_i(\mu\text{F})$	100
$C_o(\mu\text{F})$	100
$F_s(\text{KHz})$	10

Simulation results with constant radiation at 1000W/m^2 and varying temperature of 25, 50 and 75°C are studied. Fig.22 shows the array output power under MPPT conditions. It is obvious that the available power is extracted. Armature voltage, current and the duty cycle ratio of boost converter are shown in Figs. 23, 24 and 25 respectively. Fig. 26 shows the speed of the motor and the torque is shown in Fig. 27. The results show a very good performance for the system operating with MPPT and an acceptable output voltage ripple around 4 V (3.3%). The duty cycle of the converter matches approximately the optimum duty cycle obtained from steady state analysis. For better comparison the duty cycle obtained from steady state and simulation results are tabulated in Table 4.

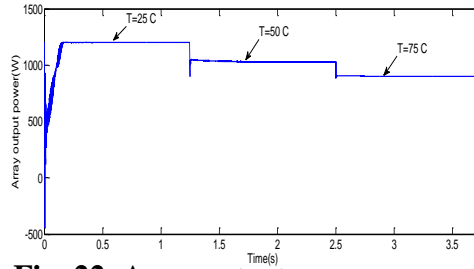


Fig. 22. Array output power response

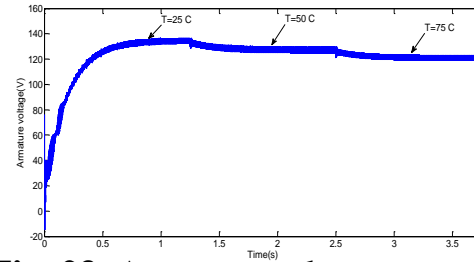


Fig. 23. Armature voltage response

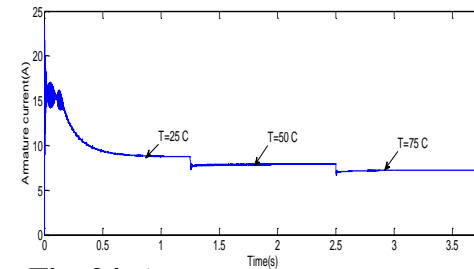


Fig. 24. Armature current response

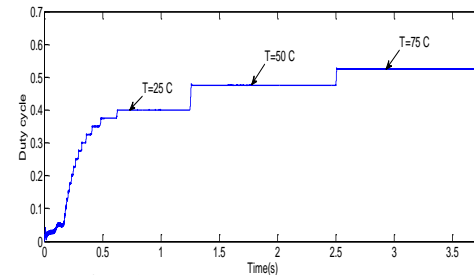


Fig. 25. Duty cycle response

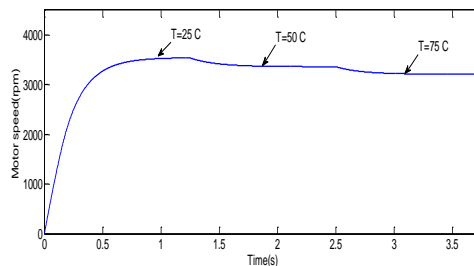


Fig. 26. Motor speed response

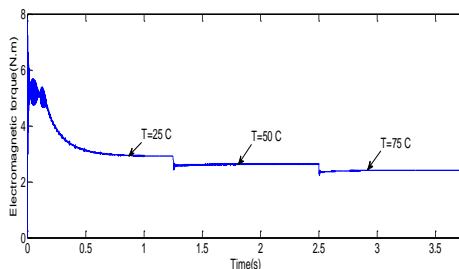


Fig. 27. Torque response

Table 4.

Duty cycle ratio comparison between steady state and simulation results under different temperatures

Temperature(°C)	Steady state (%)	Simulation result (%)
25	41.6	40
50	45.9	47.5
75	50.5	52.5

System response with constant temperature at 25 °C and varying radiation of 400W/m² , 600W/m² , 800W/m² and 1000W/m² is obtained. Fig. 28 shows the array output power. Armature voltage, current and duty cycle are shown in Figs.29, 30 and 31 respectively. Fig.32 shows motor speed and the torque is shown in Fig.33. Comparison between duty cycle obtained from steady state analysis and simulation results is shown in Table 5. The results show a very good agreement between simulation and steady state response which shows the effectiveness of system MPPT under various atmospheric conditions.

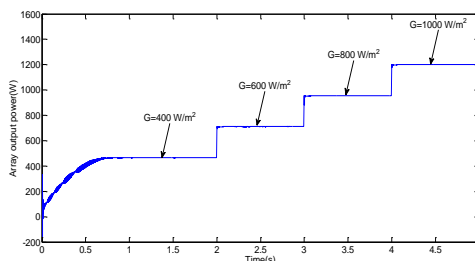


Fig. 28. Array output power response

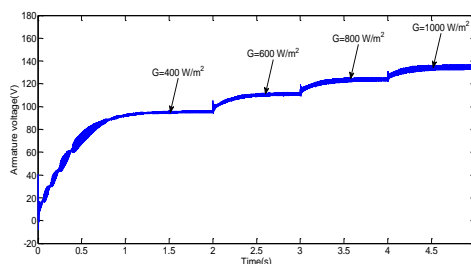


Fig. 29. Armature voltage response

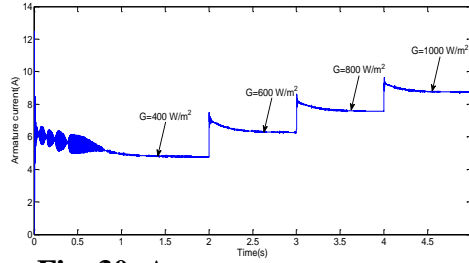


Fig. 30. Armature current response

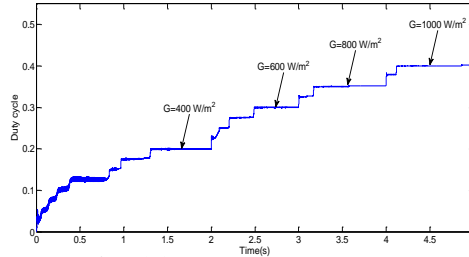


Fig. 31. Duty cycle response

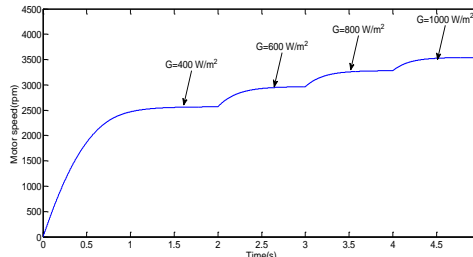


Fig. 32. Motor speed response

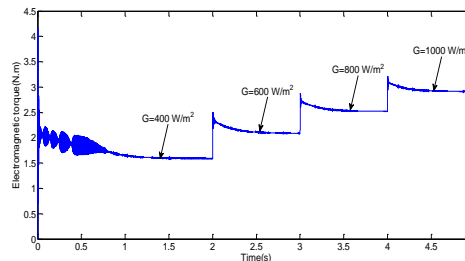


Fig. 33. Torque response

Table 5.

Duty cycle ratio comparison between steady state and simulation results under different radiations

Radiation(W/m^2)	Steady state (%)	Simulation result (%)
400	20.3	20
600	30.4	30
800	37.1	35.2
1000	41.6	40

6. Conclusion

This paper proposes an accurate model for photovoltaic water pumping system; consisting of PV generator, boost converter and PM dc motor-pump set. The system is studied under direct coupling and MPPT conditions .Optimum duty cycle ratio is obtained using simple steady state analysis by knowing the load line of the motor –pump set with simple graphical method. The system performance with different atmospheric conditions of temperature and radiation is analyzed .System under direct coupling has a low efficiency compared with that using IC MPPT method due to loss of some available power. Simulation results show a very good performance, and match approximately system solution obtained using steady state analysis under different atmospheric conditions.

REFERENCES

- [1] M. A. Elgendy, B. Zahawi, and D. J. Atkinson, "Comparison of directly connected and constant voltage controlled photovoltaic pumping systems," *IEEE Trans. Sustain. Energy*, vol. 1, no. 3, pp. 184–192, Oct. 2010.
- [2] J. Gonzalez-Llorente, E. I. Ortiz-Rivera, A. Salazar-Llinas and E. Jimenez-Brea, "Analyzing the optimal matching of DC motors to photovoltaic modules via DC-DC converters," *Applied Power Electronics Conference and Exposition(APEC), Twenty-Fifth Annual IEEE*, Palm Springs, CA, pp. 1062 – 1068, 18 march 2010.
- [3] M. A. Elgendy, B. Zahawi, D. J. Atkinson and D. Giaouris "Dynamic behaviour of DC motor-based photovoltaic pumping systems under searching MPPT algorithms," *POWERENG 2009*, Lisbon, Portugal, March 18 -20 ,2009, pp 413-418 .
- [4] T. Eswam and P. L. Chapman, "Comparison of photovoltaic array maximum power point tracking techniques," *IEEE Trans. Energy Convers.*, vol. 22, no. 2, pp. 439–449, Jun. 2007.
- [5] M. A. Elgendy, B. Zahawi, and D. J. Atkinson, "Analysis of the performance of DC photovoltaic pumping systems with maximum power point tracking," in *Proc. IET Int. Conf. Power Electronics, Machines and Drives*, York, U.K., 2008, pp. 426–430.
- [6] A. Tariq and M. Asghar, "Matching of a separately excited DC motor to a photovoltaic panel using an analog maximum power point tracker," *IEEE International Conf. on Industrial Technology ICIT 2006, Mumbai*, pp. 1020–1025, Dec. 2006.
- [7] M. A. Elgendy, B. Zahawi, and D. J. Atkinson, "Assessment of the incremental conductance maximum power point tracking algorithm," *IEEE Trans. Sustain. Energy*, vol. 4, no. 1, pp. 108–117, Jan. 2013.
- [8] A. Safari and S. Mekhilef, "Simulation and hardware implementation of incremental conductance MPPT with direct control method using cuk converter," *IEEE Trans. Ind. Electron.*, vol. 58, no. 4, pp. 1154–1161, Apr. 2011.
- [9]- D. Sera, R. Teodorescu, and P. Rodriguez, "PV panel model based on data sheet values", *IEEE International Symposium on Industrial Electronics ISIE 2007, Vigo, Spain*, pp. 2392-2396, September-2007.
- [10]- A. K. Sinha, V. Mekala, and S. K. Samantaray, "Design and testing of PV maximum power tracking system with MATLAB simulation" in *Proc. IEEE Region 10 Conf., Fukuoka*, Nov. 2010, pp. 466–473.
- [11] G.El-Saady, El-Nobi A.Ibrahim, Mostafa Ahmed, "Modeling and maximum power point tracking with ripple control of photovoltaic system", *MEPCON'14, the international middle east power systems conference*, Cairo, Egypt, Dec. 2014.
- [12] N. Mohan, T. M. Undeland, and W. P. Robbins, "Power Electronics, Converters Applications and Design, 2nd Edition", Book, *John Wiley & Sons, Inc.*, 1995, pp. 172-178.
- [13] B. M. Hasaneen and Adel A. Elbaset Mohammed, "Design and simulation of dc-dc boost converter", *Power System Conference, Aswan, Egypt*, 2008, *MEPCON 2008, 12th International Middle-East*.

- [14] M. Kolhe, J. C. Joshi, and D. P. Kothari, "Performance analysis of a directly coupled photovoltaic water-pumping system", *IEEE Trans. on energy conversion*, vol. 19, no. 3, sep. 2004.
- [15] K. Venkatesan and D. Cheverez-Gonzalez, "Matching dc motors to photovoltaic generators for maximum power tracking", *Applied Power Electronics Conf. and Exp. APEC '97 Conf. Proc. 1997., Atlanta, GA 12th Annual*, vol. 1 pp. 514-519, Feb. 1997.
- [16] A. B. Raju, S. R. Karnik and R. Jyoti, "Maximum efficiency operation of a single stage inverter fed induction motor PV water pumping system", *First International Conference on Emerging Trends in Engineering and Technology*, pp. 905–910, Nagur, India, 16–18 July 2008.
- [17] Hamid M. B. Metwally and Wagdy R. Anis, "Dynamic performance of directly coupled photovoltaic water pumping system using D.C. shunt motor", *Energy Convers. Mgmt*, Vol. 37, No. 9, pp. 1407-1416, 1996.
- [18] Pallavee Bhatnagar, R .K. Nema, "Maximum power point tracking control techniques: State-of-the-art in photovoltaic applications", *Renewable and Sustainable Energy Reviews* 23, pp. 224–241, 2013.
- [19] M. Salhi, R. El-Bachtiri, and E. Matagne, "The development of a new maximum power point tracker for a PV panel", *International Scientific Journal for Alternative Energy and Ecology (ISJAE)*, vol. 62, no.6, pp. 138-145, 2008.

الأداء الأمثل لنظام رفع المياه باستخدام الطاقة الشمسية تحت ظروف التشغيل المختلفه

الملخص العربي:

تقدم هذه المقالة نظام رفع المياه. ويتكون من خلايا شمسية ورافع للجهد المستمر ومحرك ذو مغناطيس دائم مربوط بمضخة رفع المياه. جميع أجزاء النظام تم نمذجتها. متغيرات الخلايا الشمسية تم استخراجها بناء على ورقه البيانات. صمم رافع الجهد المستمر ليعمل في منطقه التوصيل المستمر ويتم التحكم فيه بطريقه تدرج الموصلية لتتبع نقطه قيمه العظمى للقدره. تم بناء النظام على برنامج المحاكاه ماتلاب. النظام المقدم درس تحت ظروف الربط المباشر و تتبع نقطه قيمه العظمى للقدره وأظهرت النتائج أداء جيد جدا للنظام تحت العمل بطريقه تتبع النقطه العظمى للقدره مقارنة بالربط المباشر. النظام تم اختباره تحت ظروف متغيره من درجه الحراره والأشعاع .